ACCELERON AEROSPACE JOURNAL (AAJ)
E-ISSN: 2583-9942 (Online) | Accessible at www.acceleron.org.in

Volume 5, Issue 1, (pp.1224-1230)
Article ID: AAJ.11.2106-2537
Research Paper
https://doi.org/10.61359/11.2106-2537

Supersonic Aerodynamic Analysis of a High Performance Reconnaissance Aircraft via CFD

Sadiq Ali Mir*, Suhana Arsh†, Rishika Bandyopadhyay‡, Tushar Mongia§

R V College of Engineering, Aerospace Engineering, Bengaluru, India.

Abstract: Modern advancements in aerospace engineering have accelerated the development of high-performance, stealthy reconnaissance aircraft. This research delves into the aerodynamic performance of such an aircraft operating at supersonic speeds. Through advanced computational tools, we explore the complex interplay of aerodynamic forces acting on this type of aircraft during critical reconnaissance missions. A key aspect of this research is the analysis of a digital model resembling a modern, high-speed reconnaissance aircraft designed for minimal radar signature. This model will be subjected to rigorous aerodynamic analysis using established computational techniques. By examining the flow characteristics around the aircraft at Mach 3, the study aims to gain valuable insights that can contribute to the optimization of future stealthy reconnaissance vehicles. Understanding the challenges associated with maintaining stability, maneuverability, and fuel efficiency at such extreme velocities is paramount for successful reconnaissance operations. This research provides a crucial step towards achieving this goal, ultimately contributing to the development of more advanced and effective high-speed, stealthy reconnaissance aircraft.

Table of Contents

1. Introduction

Modern aerial reconnaissance plays a critical role in national security, providing vital intelligence during high-stakes missions in contested airspace. To effectively fulfill this role, reconnaissance aircraft require a delicate balance of three key characteristics: speed, stealth, and aerodynamic efficiency. Supersonic speeds enable these platforms to cover vast distances quickly, maximizing mission effectiveness. Stealth, achieved through meticulously designed shapes and advanced materials, minimizes radar signatures, making these aircraft virtually invisible to enemy detection systems. Finally, aerodynamic efficiency ensures optimal fuel consumption during long-range missions. The SR-71 Blackbird, a legendary aircraft of the Cold War era, stands as a testament to this delicate balance. Developed by Lockheed Skunk Works and operational from 1964 to 1998, the SR-71 revolutionized aerial reconnaissance [1]. This remarkable aircraft achieved unmatched performance at supersonic speeds exceeding three times the speed of sound [2]. The SR-71's success stemmed from its unique design, incorporating innovative concepts like variable-sweep wings and advanced materials like titanium, all meticulously optimized for both stealth and supersonic flight. A critical aspect of the SR-71's effectiveness was its diverse mission profile. These high-speed, high-altitude reconnaissance flights could span up to 2,575 miles (4,145 km) [8]. Depending on the target and mission requirements, the SR-71 could employ either a single-legged mission, involving a direct flight to the target area at Mach 3.0 with aerial refueling upon return, offering simplicity but limited range; or a multi-legged mission with strategically placed aerial refueling stops, enabling the SR-71 to reach more distant targets while maintaining high speeds throughout the mission. The following table summarizes the key specifications of the SR-71 Blackbird, which serve as a reference point for the high-performance reconnaissance aircraft. The complex interplay of aerodynamic forces acting on the SR-71 at such extreme velocities is paramount for achieving successful reconnaissance missions. Factors such as lift generation, drag minimization, and maintaining stability at supersonic speeds are crucial for effective operation [3]. This research delves into these aerodynamic characteristics using advanced computational tools, focusing on the SR-71 Blackbird as a model for high-speed, stealthy reconnaissance aircraft.

*R V College of Engineering, Aerospace Engineering, Bengaluru, India. **Corresponding Author:** sadiqalimir.ae21@rvce.edu.in.
†R V College of Engineering, Aerospace Engineering, Bengaluru, India. **Contact:** suhanaarsh.ae22@rvce.edu.in.
‡R V College of Engineering, Aerospace Engineering, Bengaluru, India. **Contact:** rishikab.ae22@rvce.edu.in.
§R V College of Engineering, Aerospace Engineering, Bengaluru, India. **Contact:** tusharmongia.ae22@rvce.edu.in.
Article History: Received: 07-July-2025 || Revised: 12-July-2025 || Accepted: 20-July-2025 || Published Online: 30-July-2025.

2. Methodology

This research employs a two-stage computational approach to analyze the aerodynamic performance of the SR-71 Blackbird at Mach 3. The first stage focuses on geometric modeling using OpenVSP software. OpenVSP's user-friendly interface and efficient mesh generation capabilities make it an ideal choice for creating a high-fidelity 3D model of the SR-71 [4]. However, striking a balance between geometric accuracy and computational efficiency is crucial. A highly detailed model, while capturing the intricacies of the SR-71's design, can lead to computationally expensive simulations. Conversely, an overly simplified model may not accurately represent the aircraft's geometry, potentially compromising the validity of the results. This research will achieve an optimal balance by carefully managing mesh density, particularly in critical areas like wing leading edges, while maintaining fidelity to the SR-71's unique design [5]. The NASA SC(2)-1010 supercritical airfoil was selected after conducting a comparative analysis against the RAE 2822 and the NLR 7301 airfoils using XFLR5 software. The NASA SC(2)-1010 was considered as the ideal airfoil for our case as inferred from the plots of coefficients of lift and drag against the angle of attack.

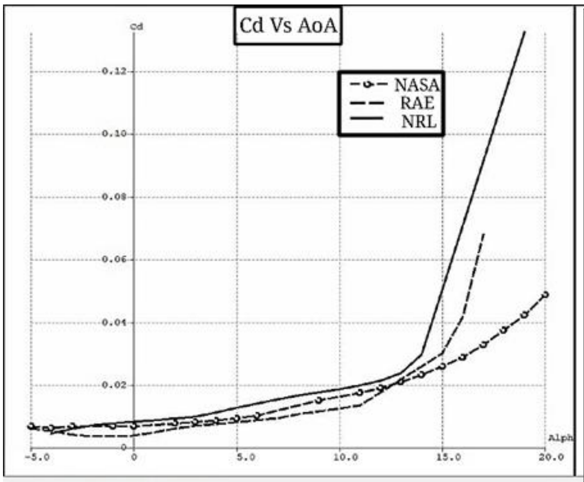

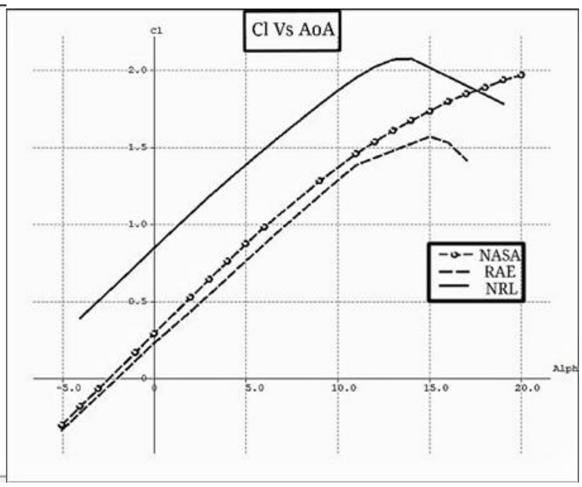

Figure 1: Cd Vs AoA

Figure 2: Cl Vs AoA

Selecting appropriate turbulence models to capture the complexities of supersonic flow is crucial. Specialized turbulence models will be chosen to account for the presence of shockwaves and boundary layer interactions characteristic of hypersonic flows [6]. Additionally, mesh generation techniques such as mesh adaptation and refinement will be employed to ensure a well-resolved computational domain around the aircraft [6]. Finally, the simulations will be run, and the results will be analyzed to extract key aerodynamic parameters such as lift coefficient (Cl), drag coefficient (Cd), and pressure distribution across the aircraft's surface. By meticulously following these steps, the CFD analysis will provide valuable insights into the aerodynamic behavior of the SR-71 Blackbird at supersonic speeds.

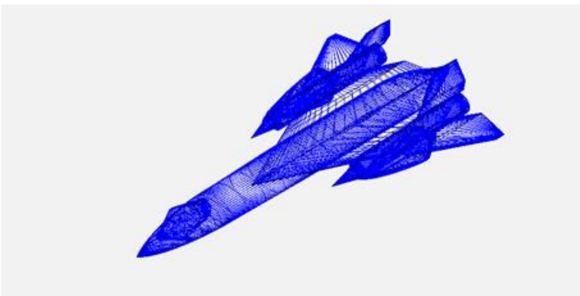

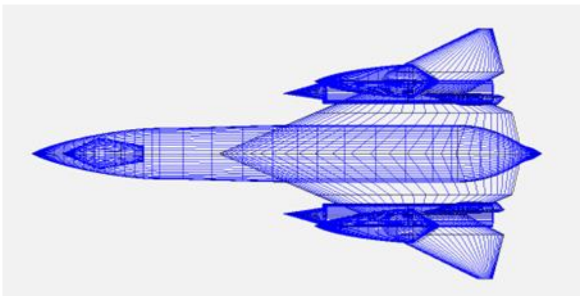

Figure 3:Design of the aircraft in OpenVSP

(Isometric View)

Figure 4:Design of the aircraft in OpenVSP

(Top View)

3. Results and Discussion

The initial phase involved a dedicated wing simulation using a high-fidelity geometric model. This analysis focused on the aerodynamic behavior of the SR-71's unique wing design at Mach 3. The primary focus was on analyzing the pressure distribution across the wing. These preliminary insights provided valuable information about

Acceleron Aerospace Journal || AAJ.11.2106-2537
Volume 5, Issue 1, pp (1224-1230)
E-ISSN- 2583-9942
https://dx.doi.org/10.61359/11.2106-2537

potential areas of concern, such as excessive shockwave formation or flow separation. These observations laid the groundwork for further investigation during the subsequent, more comprehensive CFD analysis stage.

The second stage of the research leveraged a powerful commercial CFD software package to conduct in-depth simulations of the entire SR-71 aircraft at Mach 3. These simulations aimed to capture the intricate flow phenomena surrounding the aircraft in its hypersonic environment. The analysis focused on three key aerodynamic parameters: lift and drag coefficients (Cl and Cd), and pressure distribution. Lift and drag coefficients provided valuable insights into the SR-71's ability to generate lift for stable flight and the amount of drag experiences, respectively. These coefficients will be compared to available experimental data or established theoretical models for hypersonic aerodynamics. Any deviations from expected values will prompt further investigation into potential sources of error, such as limitations of the turbulence models used in the simulations or inaccuracies in the geometric model of the SR-71. A critical aspect of the analysis involved visualizing and interpreting the pressure distribution across the entire surface of the SR-71. Pressure variations play a significant role in determining the aerodynamic forces acting on the aircraft. High-pressure regions on the underside of the wings contribute to lift, while pressure differentials between the leading and trailing edges are crucial for maintaining control authority. By analyzing the pressure distribution, the study can identify areas of concern, such as excessive shockwave formation or flow separation. These insights will be instrumental in understanding the challenges associated with hypersonic flight and paving the way for design improvements in future hypersonic vehicles.

3.1 Simulations

The CFD simulations employed a two-software approach, leveraging the strengths of Ansys Fluent and Siemens Simcenter FloEFD for comprehensive analysis of the high-performance reconnaissance aircraft's aerodynamic performance at Mach 3. Ansys Fluent provided a user-friendly interface and efficient handling of the complex aircraft geometry, crucial for accurate flow modeling. A density-based, viscous solver was implemented within Fluent to capture the compressible flow characteristics at supersonic speeds. This solver type is essential for accurately resolving the behavior of air at high Mach numbers, where compressibility effects become significant [8]. Siemens Simcenter FloEFD, known for its robust mesh generation capabilities and suitability for simulating complex external aerodynamic flows, was employed for mesh generation [9]. The software utilizes a hybrid unstructured mesh approach, combining tetrahedral elements in the boundary layer region with prismatic elements in the far-field. This approach offers a balance between capturing the intricate details of the near-wall flow behavior and maintaining computational efficiency in the far-field [10].

To ensure a well-resolved computational domain and capture the complex flow physics around the aircraft, particularly in critical regions like wing leading edges and the nose cone, mesh adaptivity was employed. This technique refines the mesh density in areas where significant variations in flow parameters are expected, such as shockwave formation and boundary layer growth [11]. The well-resolved computational domain obtained through these techniques paves the way for accurate analysis of the flow characteristics around the aircraft in the subsequent sections.

3.2 Analysis

The CFD simulations generated a wealth of data pertaining to the aerodynamic performance of the high-performance reconnaissance aircraft at Mach 3 and 0 degrees angle of attack (AoA). This section delves into the analysis of this data, focusing on key parameters that govern the aircraft's flight characteristics.

3.2.1 Overall Aircraft Performance

The analysis begins with examining the overall pressure, Mach number, and velocity distributions around the entire aircraft. These visualizations provide a holistic understanding of the flow behavior at supersonic speeds. Pressure distribution plots reveal areas of high and low pressure, which are crucial for understanding lift generation and drag forces acting on the aircraft, as detailed in . Mach number contours illustrate the regions where the flow surpasses the speed of sound (Mach 1), while velocity plots depict the magnitude and direction of the airflow around the aircraft.

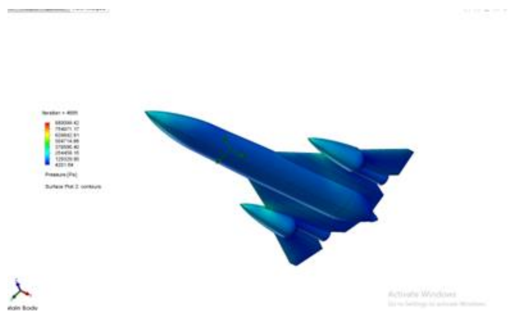

Figure 6: Pressure plot at 0 angle of attack

Figure 7: Lift force plot at 0 angle of attack

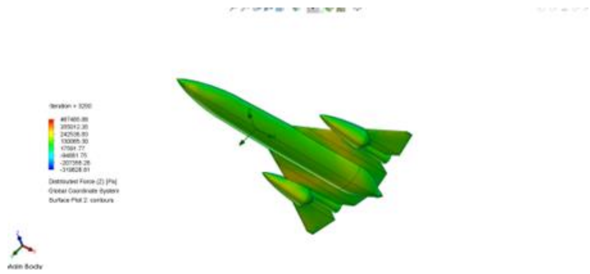

Figure 8: Pressure plot at 87 angle of attack

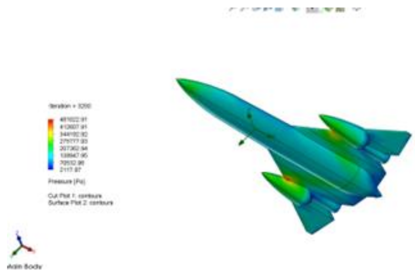

Figure 9: Lift force plot at 7 angle of attack

3.2.2 Wing airfoil Aerodynamic Characteristics

For a detailed understanding of the chosen airfoil's performance, a dedicated analysis is conducted using Ansys Fluent. Here, a specific airfoil profile, such as the NASA SC (2) - 1010, is isolated and subjected to individual simulations at Mach 3. Ansys Fluent robust capabilities allow for the extraction of vital aerodynamic coefficients, including lift coefficient (Cl) and drag coefficient (Cd). These coefficients quantify the lift and drag forces generated by the airfoil at a 0, 2 and 7 degrees AoA.

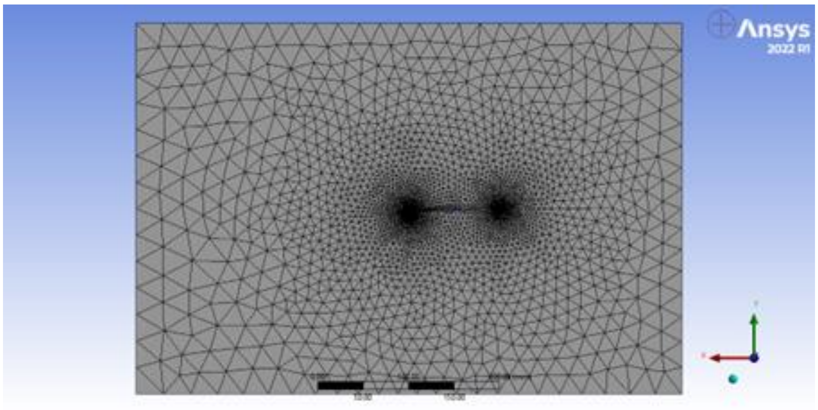

Figure 10: Mesh Quality

For the meshing of the wing, a rectangular domain with dimensions 0.3 m × 0.2 m × 0.2 m was utilized. This domain encompasses 188,117 nodes and 1,085,037 elements, ensuring a detailed and accurate computational grid. The element size for the general domain is set to 30 mm. However, for the wing, a finer element size of 20 mm is used, incorporating proximity refinement to capture intricate details and enhance the accuracy of the aerodynamic analysis.

At 0 degree angle of attack

Check for updates
Acceleron Aerospace Journal || AAJ.11.2106-2537
Volume 5, Issue 1, pp (1224-1230)
E-ISSN- 2583-9942
https://dx.doi.org/10.61359/11.2106-2537

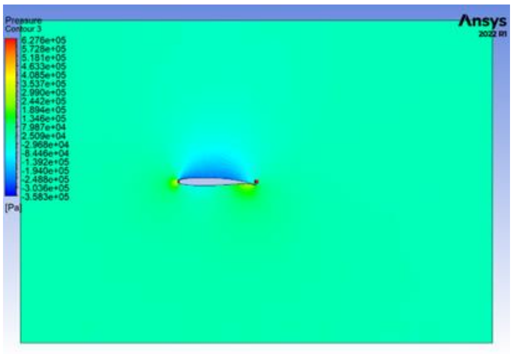

Figure 11: Pressure plot at Mach 3

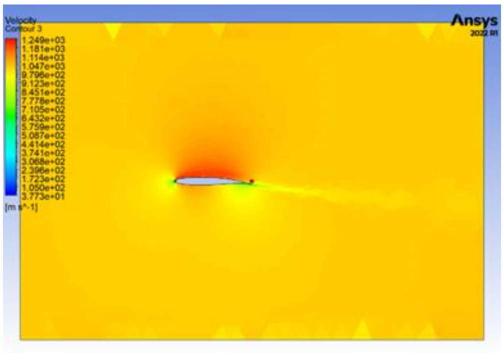

Figure 12: Velocity plot at Mach 3

At 2-degree angle of attack

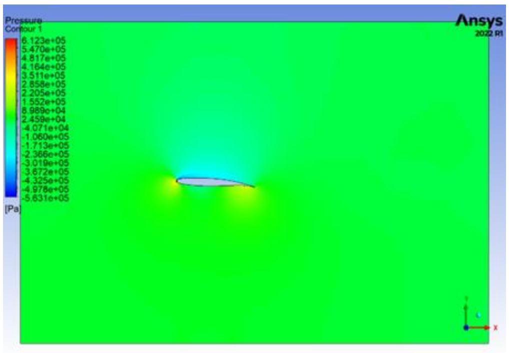

Figure 13: Pressure plot at Mach 3

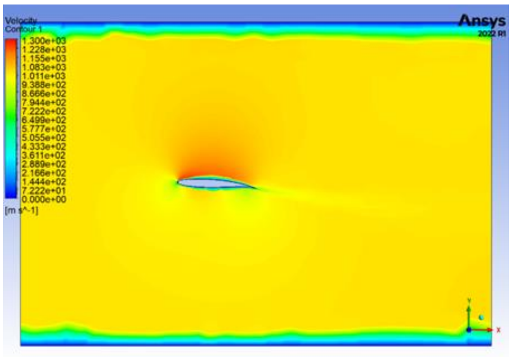

Figure 14: Velocity plot at Mach 3

At 5-degree angle of attack

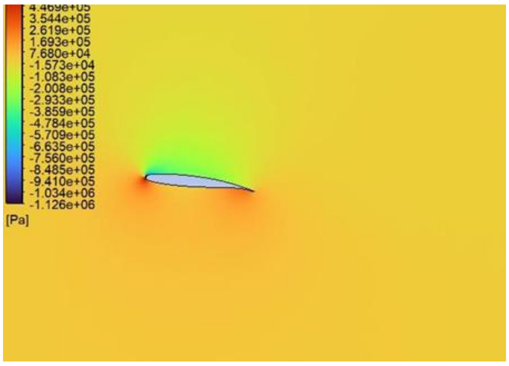

Figure 15: Pressure plot at Mach 3

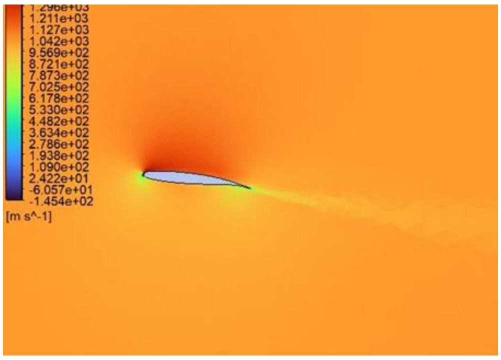

Figure 16: Velocity plot at Mach 3

At 7-degree angle of attack

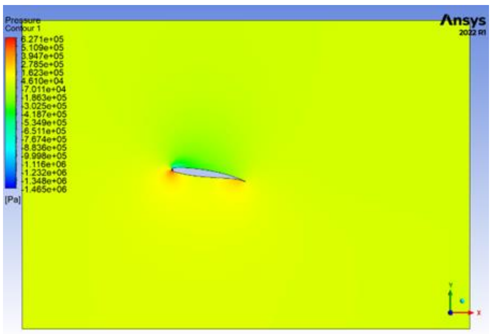

Figure 17: Pressure plot at Mach 3

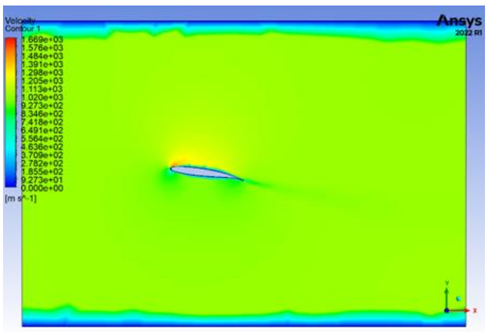

Figure 18: Velocity plot at Mach 3

Table-1: Comparison of various parameters for different angle of attacks

Sl. No	Angle of Attack (Degree)	Velocity (m/s)	C_l (Lift Coefficient)	C_d (Drag Coefficient)	C_m (Moment Coefficient)	Lift force (N)	Drag force (N)
1	0	1029	0.8413	0.00821	-0.1516	1911.31	172.720
2	2	1029	1.0662	0.00922	-0.1512	2505.66	271.732
3	5	1029	1.3827	0.01266	-0.1459	3286.12	428.345
4	7	1029	1.5815	0.01531	-0.1403	3784.13	558.714

The results show a clear correlation between AoA and the generated aerodynamic forces. As Aloe increases from 0° to 7°, Cl increases from 0.8413 to 1.5815, indicating a rise in lift force (1911.31 N to 3784.13 N). Similarly, Cd exhibits a rise with increasing AoA (0.00821 to 0.01531), leading to a corresponding increase in drag force (172.720 N to 558.714 N). The moment coefficient (Cm) displays a minor negative trend across all AoA.

3.2.3 Pressure and Temperature Distribution

The analysis extends beyond the wing to examine the pressure and temperature distribution across the length of the fuselage. These parameters are crucial for understanding the overall aerodynamic efficiency of the aircraft. High-pressure regions along the fuselage can contribute to parasitic drag, while temperature variations can impact the structural integrity of the aircraft skin, particularly at supersonic speeds [8]. The increased entropy at elevated temperatures can lead to increased friction resulting in drag. Additionally, the vorticity plot maps the locations of vortex generation along the fuselage length which can be used for further design enhancement to minimize vortex drag and increase overall lift generation. Owing to the shear loads exerted by the supersonic winds on the aircraft skin, the resulting shear stress along the fuselage is illustrated in the shear stress plot.

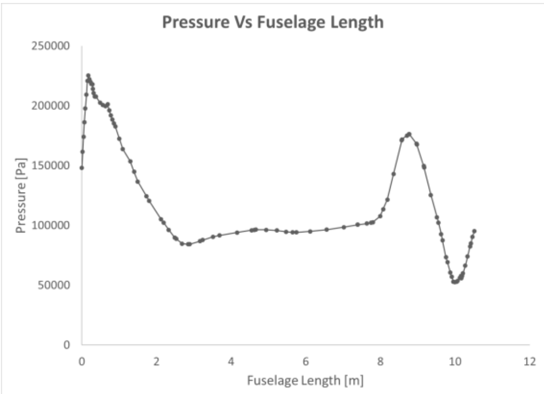

Figure 19: Pressure Vs Fuselage Length

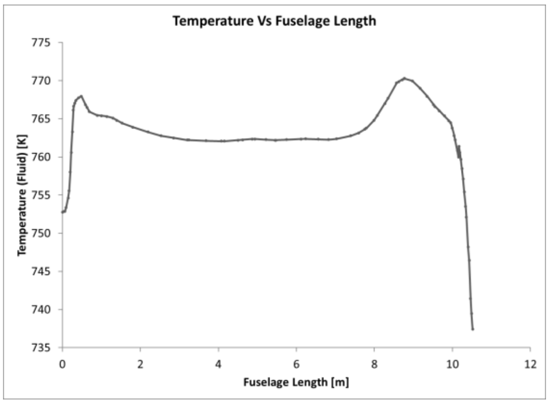

Figure 20: Temperature Vs Fuselage Length

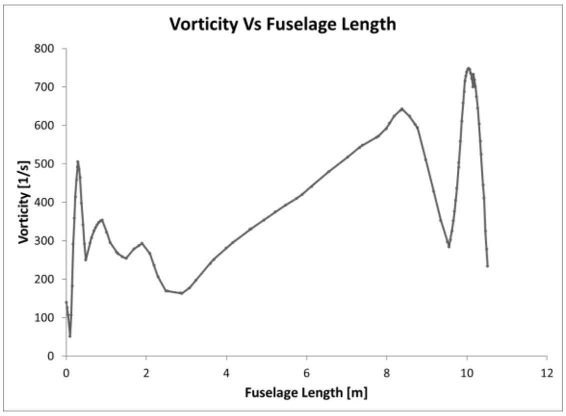

Figure 21: Vorticity Vs Fuselage Length

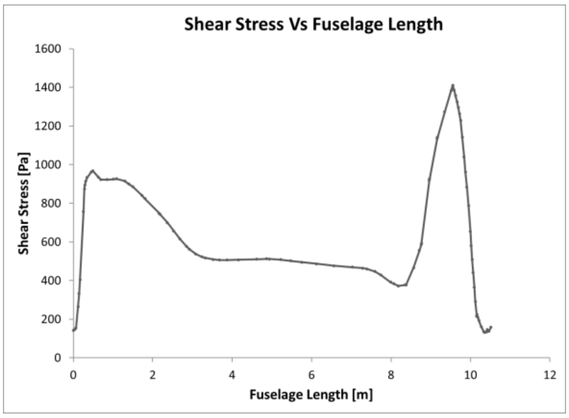

Figure 22: Shear Stress Vs Fuselage Length

4. Conclusion

This research employed CFD simulations to investigate the aerodynamic performance of a high-performance reconnaissance aircraft modeled after the SR-71 Blackbird at Mach 3. The analysis focused on key aerodynamic parameters like lift coefficient (Cl), drag coefficient (Cd), pressure distribution, and temperature variations. The results revealed a positive correlation between angle of attack (AoA) and lift generation, with Cl increasing from 0.8413 to 1.5815 as AoA rose from 0° to 7°. However, this rise in lifts came at the cost of increased drag (Cd rising from 0.00821 to 0.01531). The pressure and temperature distributions across the fuselage provided valuable insights into potential areas for design optimization to minimize parasitic drag and ensure structural stability during supersonic flight. These findings contribute to the ongoing development of high-performance, stealthy reconnaissance aircraft by highlighting the complex interplay of aerodynamic forces at hypersonic speeds. Future research can explore advanced design modifications to achieve a more optimal balance between lift, drag, and stability for superior reconnaissance capabilities.

5. Acknowledgement

We express our sincere gratitude to **Dr. Ravindra S. Kulkarni**, Professor and Head of the Department of Aerospace Engineering, RV College of Engineering, for their invaluable support and guidance.

6. References

[1] Davies, R. E. (2010). SR-71 Blackbird: Stories from the world's fastest jet. Zenith Imprint.
[2] Goodspeed, C. A. (2003). A supersonic reconnaissance aircraft: The SR-71 Blackbird. NASA History Division. https://www.nasa.gov/gallery/sr-71-blackbird/
[3] Torenbeek, E. G. (2013). Advanced aircraft design: Conceptual design, analysis and optimization of subsonic civil airplanes (3rd ed.). John Wiley & Sons.
[4] Hsu, C.-J., Liu, H.-C., & Zing, J.-Y. (2014). Parametric design and analysis of a supersonic business jet using OpenVSP. Chinese Journal of Aeronautics, 27(1), 273–282.
[5] Anderson, J. D. (2007). Fundamentals of aerodynamics (5th ed.). McGraw-Hill Education.
[6] Wilcox, D. C. (2006). Turbulence modeling for CFD (Vol. 3). DCW Industries.
[7] Chun, K. H., & Byun, H. S. (2010). Aerodynamic optimization of a supersonic business jet fuselage for wave drag reduction. Journal of Aircraft.
[8] Hirsch, C. (2007). Numerical computation of internal and external flows: The fundamentals of computational fluid dynamics. John Wiley & Sons.
[9] Siemens Digital Industries Software. (2023). Simcenter FloEFD – Overview [Online]. https://plm.sw.siemens.com/en-US/simcenter/fluids-thermal-simulation/floefd/
[10] Spalart, P. R., & Allmaras, S. R. (1992). A one-equation turbulence model for aerodynamic flows. AIAA Paper, 92-0430.
[11] Wilcox, D. C. (2006). Turbulence modeling for CFD (3rd ed.). DCW Industries.

7. Conflict of Interest

The author declares no competing conflict of interest.

8. Funding

No funding was issued for this research.